J. Phys. Chem. A **2003,** *107,* 1879−1886

Gas Phase Generation of HCCCS and CCCHS Radicals from Anionic Precursors. The Rearrangement of CCCHS to HCCCS. A Joint Experimental and Theoretical Study

Salvatore Peppe, Suresh Dua, Andrew M. McAnoy, and John H. Bowie*
Department of Chemistry, The University of Adelaide, South Australia, 5005

Received: October 29, 2002

Theoretical studies at the CCSD(T)/aug-cc-pVDZ//B3LYP/aug-cc-pVDZ level of theory indicate that there are four stable radicals with CCC bond connectivity on the C_3HS potential surface, namely, HCCCS, CCHCS, CCCHS, and (*cyclo*-C_3H)=S. Of these structures, two have been synthesized by one electron vertical oxidation of precursor anions, formed as follows: (i) $CH_3{-}C{\equiv}C{-}S{-}C_2H_5 + O^{-\bullet} \rightarrow (HCCCS)^- + H_2O + C_2H_5^\bullet$ and (ii) $Me_3Si{-}C{\equiv}C{-}CH$(*cyclo*-SCH_2CH_2S) + $F^- \rightarrow {}^-C{\equiv}C{-}CH{=}S + Me_3SiF$ + *cyclo*-SC_2H_4. A comparison of the $^-CR^+$ and $^-NR^+$ spectra of these two anions indicate that the neutral HCCCS is stable with a lifetime of at least 1 μs, whereas the oxidation of $(CCCHS)^-$ leads to two neutrals, CCCHS and HCCCS. Theoretical calculations indicate that the rearrangement of CCCHS to HCCCS can occur by three pathways; concerted H or S rearrangements or the stepwise H rearrangement process CCCCHS → CCHCS → (*cyclo*-C_3H)=S → HCCCS. Comparison of the $^-CR^+$ and $^-NR^+$ spectra of $(CC^{13}CHS)^-$ indicates that at least a part of the rearrangement involves the S migration pathway. Theoretical considerations suggest that H rearrangement should compete with S rearrangement: there is no experimental evidence to confirm or refute this proposal.

Introduction

Comparatively few sulfur-containing molecules have been detected within interstellar or circumstellar regions of space.[1] The carbon sulfide neutrals CS, C_2S, and C_3S have been detected in the taurus molecular cloud (TMC-1)[2,3] and within the circumstellar envelope of the carbon-rich star IRC + 10216.[3,4] The polycarbon sulfides C_4S and C_5S have been characterized spectroscopically.[5] C_4S has been proposed as a plausible interstellar species,[3] whereas there has been a tentative assignment of C_5S within IRC + 10216.[3]

The cosmic abundance of elemental sulfur is 1.5 orders of magnitude below that of oxygen;[5] yet, within TMC-1, C_2S and C_3S occur at surprisingly large abundances with respect to the corresponding oxygen-containing analogues C_2O and C_3O.[6,7] This suggests that the synthetic pathways that form C_2S and C_3S may be more efficient than those that produce the oxygen analogues. A number of synthetic pathways to form polycarbon sulfides in a stellar environment have been proposed:[8−15] for example, that involving the capture of S by HCCC[15] or the reaction between the acetylene radical cation and CS to form C_3S,[11] viz (a) $C_2H_2^{+\bullet} + CS \rightarrow HCCCS^+ + H^\bullet$ and then (b) $HCCCS^+ + e \rightarrow CCCS + H^\bullet$, seem possible scenarios. In the latter case, step b is endothermic by 63.5 kcal mol^{-1}.[11] This suggests that neutral HCCCS may have a significant lifetime if its energy upon electron capture is lower than the dissociation threshold, which in turn suggests that it is possible that radical HCCCS may be present in the stellar environment.

Neutral HCCCS has been generated by pulsed discharge in a supersonic free jet of argon diluted with a mixture of acetylene and carbon disulfide.[16] Rotational spectra indicate a linear $^2\Pi$ ground state state for HCCCS,[16] consistent with theoretical calculations at the QCISD[17] level of theory.

We have previously used neutralization of charged precursors, followed by the formation of either positive or negative ions from the corresponding neutrals as a probe to detect and determine the structures of neutrals formed by vertical Franck−Condon processes. This neutralization-reionization (NR) technique was introduced by McLafferty[18] and subsequently developed by others.[19,20] In a previous NR study,[21] we reported the preparation of the radicals HCCCO and CCCHO from charged precursors in a collision cell of a mass spectrometer and showed that, although HCCCO and CCCHO are stable, some rearrangement of CCCHO to HCCCO occurred under the conditions of the neutralization experiment used to form CCCHO.[21]

Following the earlier study of HC_3O isomers,[21] this paper reports the formation of the neutral radicals HCCCS and CCCHS from anion precursors of known bond connectivity and investigates, using both experimental and theoretical methods, whether these neutrals decompose or rearrange under the experimental conditions used to effect the neutralization process.

Experimental Section

A. Mass Spectrometric Methods. For a detailed description of the experiment and the instrument used, see ref 21. In brief, the experiments were performed using a two-sector modified VG ZAB 2HF mass spectrometer with BE configuration, where B and E represent magnetic and electric sectors, respectively. The precursor anion to HCCCS was formed in the chemical ionization ion source by a standard $O^{-\bullet}$ (formed by dissociative resonance capture of nitrous oxide[22]) reaction as shown in eq 1. The precursor anion to CCCHS was formed in the chemical ionization source, utilizing the sequence shown in eq 2, which involves an S_N2 (Si) reaction (using F^- from SF_6[23]) of a type first reported by DePuy[24]

$$CH_3{-}C{\equiv}C{-}S{-}C_2H_5 + O^{-\bullet} \rightarrow HC{\equiv}C{-}{}^-C{=}S + H_2O + C_2H_5^\bullet \quad (1)$$

---

* To whom correspondence should be addressed. E-mail: john.bowie@adelaide.edu.au.

10.1021/jp022328f CCC: $25.00

$$Me_3Si{-}C{\equiv}C{-}CH\ (cyclo\text{-}SCH_2{-}CH_2S) + F^- \rightarrow {}^-C{\equiv}C{-}CH{=}S + Me_3SiF + cyclo\text{-}SC_2H_4 \quad (2)$$

Typical source conditions were as follows: source temperature 200 °C, repeller voltage −0.5 V, ion extraction voltage 7 kV, and mass resolution $m/\Delta m \geq 1500$. Each neutral precursor was inserted into the ion source through the septum inlet, which was was heated to 60 °C to give a measured pressure of ca. 10^{-6} Torr inside the source housing. The reagent gas [either N_2O (for $O^{-\bullet}$) or SF_6 (for F^-)] was introduced through a gas inlet into the ion source, to give a measured total pressure of ca. 10^{-5} Torr in the source housing. The estimated total pressure in the ion source is 10^{-1} Torr.[25] Collisional induced (CID) spectra of $HCCCS^-$ and ^-CCCHS were determined using B to select m/z 69 in each case and utilizing argon as the target gas in the first collision cell following B. The pressure of argon in the first cell was maintained such that 80% of the parent ion beam was transmitted through the cell. This corresponds to an average of 1.1−1.2 collisions per ion.[26] Product anion peaks resulting from CID processes were recorded by scanning E.

Neutralization−reionization[18−20] ($^-NR^+$) experiments were performed for mass-selected anions utilizing the dual collision cells located between the magnetic and electric sectors. Neutralization of anions was effected by collisional electron detachment using O_2 at 80% transmittance (of the main beam) as the collision gas in the first collision cell, whereas reionization to cations was achieved by collision of the neutrals with O_2 (80% transmittance) in the second collision cell. To detect a reionization signal due to the parent neutral, the neutral species must be stable for the one microsecond time frame of this experiment. Charge reversal ($^-CR^+$) spectra[27,28] were recorded using single collision conditions in collision cell 1 (O_2, 80% transmission of main beam).

B. Synthetic Procedures. *(a) 1-(Thioethoxy)-1-propyne* ($CH_3{-}C{\equiv}C{-}S{-}C_2H_5$). 1-(Thioethoxy)-1-propyne was prepared by a reported method.[29]

(b) [2−1,3-Dithiolan-3-yl-1-ethylnyl]trimethylsilane [$Me_3Si{-}C{\equiv}C{-}CH(cyclo\text{-}SCH_2{-}CH_2S)$]. [2−1,3-Dithiolan-3-yl-1-ethylnyl]trimethylsilane was prepared by an adaptation of the method of Furth et al.[30] Boron trifluoride etherate (899 mg) was added dropwise to a stirred solution of trimethylsilyl propiolaldehyde (9 cm^3) and 1,2-ethanedithiol (205 mg) in dichloromethane (9 cm^3) and methanol (9 cm^3) at 0 °C. The mixture was allowed to stir at 20 °C for 6 h, quenched with aqueous sodium hydrogen carbonate (saturated, 15 cm^3), and then extracted with diethyl ether (10 cm^3 × 3), and the organic layer was separated and washed with aqueous sodium hydrogen carbonate (saturated, 15 cm^3) and aqueous sodium chloride (saturated, 15 cm^3) and was dried ($MgSO_4$), concentrated, and distilled to give the product (yellow oil, 250 mg, 62% yield). The positive ion mass spectrum does not give a molecular cation radical. $[M - H]^-$ (ZAB 2HF instrument), found 202.032; $C_8H_{14}S_2Si$ requires 202.031. ^1H NMR, 200 MHz in $CDCl_3$; δ 0.09 (s, 9H); 2.60 (s, 4H); 5.08 (s, 1H).

(c) [2-^{13}C-2−1,3-Dithiolan-3-yl-1-ethylnyl]trimethylsilane [$Me_3C{\equiv}C{-}^{13}CH(cyclo\text{-}SCH_2{-}CH_2S)$]. This was prepared from $Me_3Si{-}C{\equiv}C{-}^{13}CHO$ by the method used for the unlabeled analogue. Trimethylsilylpropioaldehyde-^{13}C was prepared from the anion of trimethylsilylacetylene and ^{13}C labeled dimethylformamide ($^{13}C = 99\%$) by a standard method.[31]

C. Theoretical Methods. Geometry optimizations were carried out with the Becke 3LYP method[32,33] using the Dunning aug-cc-pVDZ basis set[34] basis set within the Gaussian 98 suite of programs.[35] Stationary points were characterized as either minima (no imaginary frequencies) or transition structures (one imaginary frequency) by calculation of the frequencies using analytical gradient procedures. The minima connected by a given transition structure were confirmed by intrinsic reaction coordinate (IRC) calculations. The calculated frequencies were also used to determine zero-point vibrational energies which were used as a zero-point correction for the electronic energies. We have previously reported the success of the B3LYP method in predicting geometries of unsaturated chain structures and that this method produces optimized structures, at low computational cost, that compare favorably with higher level calculations.[36] The B3LYP method provides good agreement with experimental observations of C_nS ($n = 2{-}9$) molecules.[37] More accurate energies for the B3LYP geometries were determined using the CCSD(T) method including zero-point energy correction (calculated by vibrational frequencies at the B3LYP/aug-cc-pVDZ level of theory). All calculations were carried out on the Alpha Server at the Australian Partnership for Advanced Computing (APAC) National Facility (Canberra).

Results and Discussion

Stable Neutral Isomers of C_3HS. It is possible that HCCCS and perhaps other neutral isomers with this atomic composition may be formed in stellar environs by neutral/neutral[11] or ion molecule reactions.[12] Thus, we have carried out theoretical calculations at the CCSD(T)/aug-cc-pVDZ//B3LYP/aug-cc-pVDZ level of theory to determine how many stable isomers C_3HS there are with CCCS bond connectivity. There are four stable doublet structures: their structural and energy data are recorded in Table 1. It has also been shown that there are quartet structures corresponding to HCCCS, CCCHS, and ($cyclo$-C_3H)=S, but these are significantly more positive in energy than the corresponding doublet, and we have considered them no further: viz differences in energy between the doublet and the higher energy quartet states are HCCCS (+65.6 kcal mol^{-1}), CCCHS (+39.1 kcal mol^{-1}), and [($cyclo$-C_3H)=S] (+73.1 kcal mol^{-1}) at the QCISD/6-311G**//B3LYP/6-311G** level of theory.[15]

The stable doublet structures **1** to **4** are shown in Scheme 1. The valence bond structures approximate the geometric data recorded in Table 1. The structural data given for **1** indicate an almost linear CCCS skeleton with an HCC angle of about 152°. Experimental data indicate a linear structure,[16,17] and calculations at the QCIST and higher levels of theory indicate the computed geometry is dependent upon the level of theory used.[15,17] At the CCSD(T)/aug-cc-pVDZ//B3LYP/aug-cc-pVDZ level, the four stable structures **1**−**4** occupy minima within 48 kcal mol^{-1} of each other on the doublet neutral potential surface, and all need to be considered in this study. The next task is to determine whether each of these neutrals can be formed from ionic precursors.

Stable Anion Isomers of C_3HS. In previous studies, we have generally used negative precursors to generate transient neutrals in collision cells of a mass spectrometer.[21,23] Theoretical calculations have been used to determine whether there are negative ion analogues of the neutrals **1**−**4**, and these data are recorded in Table 2. There are six stable structures on the $(C_3HS)^-$ anion potential surfaces of species containing CCCS bond connectivity. These correspond to the singlet and triplet forms of **1**, **3**, and **4**. No anionic structure **2**$^-$ (CCHCS) is stable, so doublet CCHCS is not accessible from an anion precursor. The singlet **3**$^-$ is the lowest in energy of the anionic structures (other structures are 99 to 154 kcal mol^{-1} higher in energy than **3**$^-$). The singlet structures of **3**$^-$ and **4**$^-$ are respectively 138

TABLE 1: Geometries and Energies of Neutral Isomers 1−4

	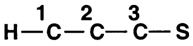 **1**	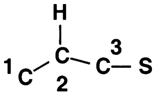 **2**	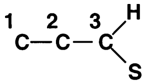 **3**	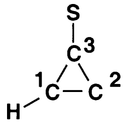 **4**
state	$^2A'$	$^2A''$	$^2A'$	$^2A'$
symmetry	C_s	C_s	C_s	C_s
energy (hartree)[a]	−512.13058	−512.05375	−512.06863	−512.10763
relative energy (kcal mol^{-1})	0	48.21	38.87	14.39
adiabatic electron affinity (eV)	6.07	8.16	7.76	6.70
dipole moment (Debye)[b]	1.24	2.00	4.04	2.42
bond length (Å)[b] or angle (°)				
C^1C^2	1.26	1.35	1.29	1.35
C^2C^3	1.31	1.38	1.37	1.47
C^1C^3				1.42
CH	1.08	1.09	1.09	1.09
C^3S	1.57	1.57	1.68	1.62
$C^1C^2C^3$	172.1	124.3	179.2	64.0
C^2C^3S	176.8	179.1	111.4	144.2
HC^1C^2	151.6			154.4
HC^2C^3		131.1		
HC^3C^2		21.4	125.0	
$C^1C^2C^3S$	180.0	0.0	180.0	
$C^2C^1C^3S$				180.0
$C^3C^1C^2S$				180.0
$C^1C^2C^3H$		180.0	0.0	
$C^1C^3C^2H$	180.0			180.0

[a] CCSD(T)/aug-cc-pVDZ level of theory including zero-point energy correction. [b] B3LYP/aug-cc-pVDZ level of theory.

TABLE 2: Geometries and Energies of Anions, 1⁻, 3⁻, and 4⁻[a]

	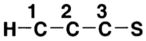		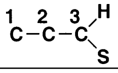		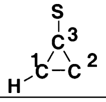	
	1s⁻	1t⁻	3s⁻	3t⁻	4s⁻	4t⁻
state	$^1A'$	$^3A''$	$^1A'$	$^3A''$	$^1A'$	$^3A''$
symmetry	C_s	C_s	C_s	C_s	C_s	C_s
energy (hartree)[b]	−512.18672	−512.18260	−512.35374	−512.13419	−512.19668	−512.10853
relative energy (kcal mol^{-1})	104.81	107.39	0.0	137.77	98.56	153.87
dipole moment (Debye)[c]	2.98	0.87	4.92	5.25	1.46	0.87
bond length (Å)[c] or angle (°)						
C^1C^2	1.34	1.30	1.27	1.29	1.40	1.35
C^2C^3	1.28	1.29	1.38	1.38	1.46	1.46
C^1C^3					1.37	1.42
CH	1.12	1.08	1.10	1.09	1.09	1.09
C^3S	1.64	1.64	1.69	1.76	1.69	1.63
$C^1C^2C^3$	171.2	172.2	174.8	178.8	64.0	60.7
C^2C^3S	177.5	178.6	129.2	109.6	149.7	154.9
HC^1C^2	111.4	140.7			146.3	154.9
HC^3C^2			115.4	127.2		
$C^1C^2C^3S$	180.0	180.0	180.0	0.0	180.0	180.0
$C^1C^2C^3H$			0.0	180.0		
$C^2C^3C^1H$					180.0	180.0
$C^3C^2C^1H$	180.0	180.0				

[a] The nomenclature 1s⁻ and 1t⁻ are used to indicate the singlet and triplet states of anion 1, respectively. [b] CCSD(T)/aug-cc-pVDZ level of theory including zero-point energy correction. [c] B3LYP/aug-cc-pVDZ level of theory.

SCHEME 1

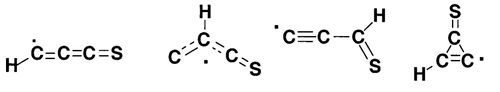

1 (0 kcal mol^{-1}) **2** (+ 48.2) **3** (+ 38.9) **4** (+ 14.4)

and 55 kcal mol^{-1} lower in energy than the corresponding triplet forms (see Table 2), whereas the singlet state of **1**⁻ is only 2.5 kcal mol^{-1} lower in energy than the triplet form. Comparison of the geometries of the doublet neutral and singlet anion structures of each of the species **1**, **3**, and **4** (Tables 1 and 2) shows that the two structures of each pair are very similar in geometry, which means that the singlet anions **1**⁻, **3**⁻, and **4**⁻ are at least theoretically, appropriate candidates for the formation of the required neutral by collision induced one-electron oxidation by a vertical Franck−Condon process.[cf.20]

Syntheses of (HCCCS)⁻ and (CCCHS)⁻ and their CID Spectra. The anions (HCCCS)⁻ and (CCCHS)⁻ were synthesized in the ion source of the mass spectrometer by the reactions shown in eqs 1 and 2 (Experimental Section). Process eq 1 involves elimination of water from $CH_3{-}C{\equiv}C{-}S{-}C_2H_5$ using the $O^{-\bullet}$ method,[22] followed by loss of $C_2H_5^{\bullet}$ to yield (HCCCS)⁻.

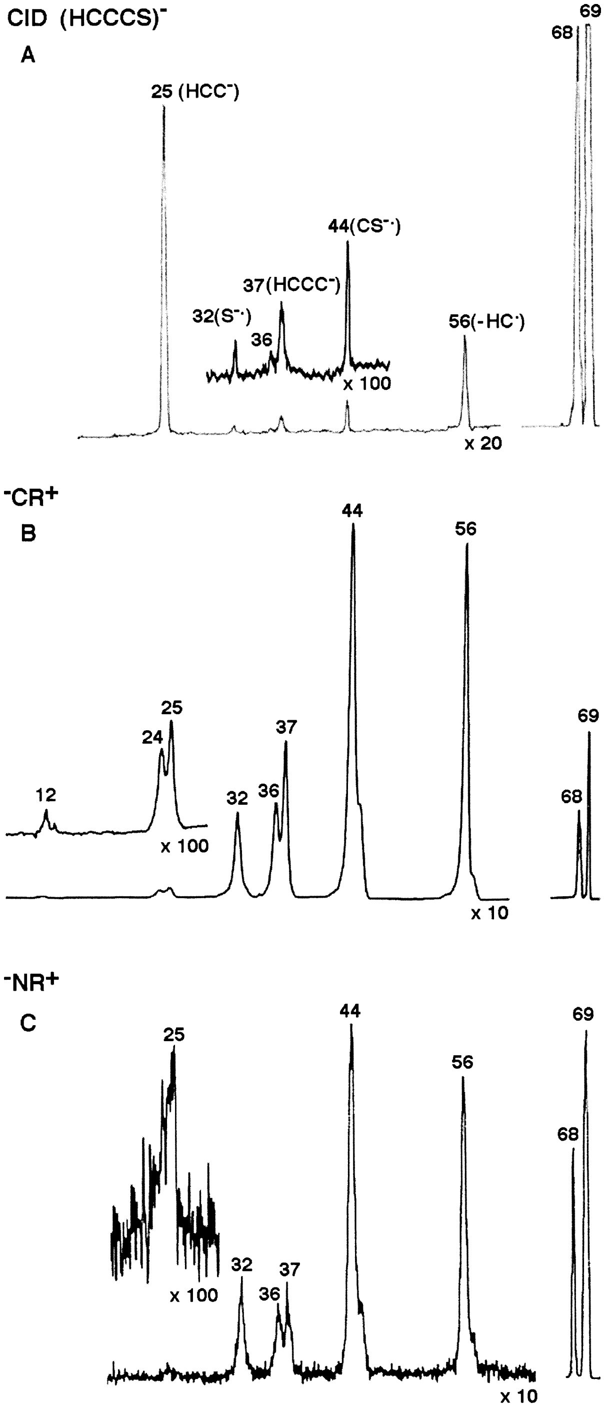

Figure 1. (A) Collision induced (CID) mass spectrum (MS/MS of $(HCCCS)^-$. (B) Charge reversal ($^-CR^+$) mass spectrum of $(HCCCS)^-$. (C) Neutralization reionization ($^-NR^+$) mass spectrum of $(HCCCS)^-$ VG ZAB 2HF mass spectrometer. For experimental conditions see Experimental Section.

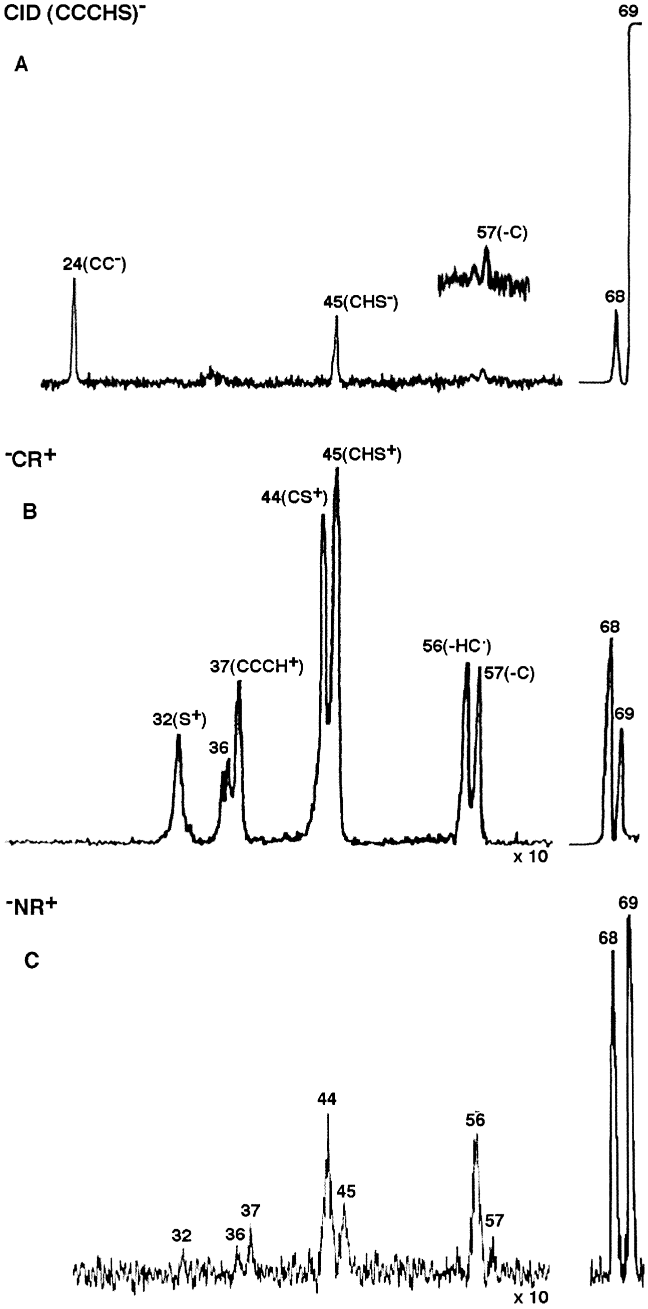

Figure 2. (A) Collision induced (CID) mass spectrum (MS/MS) of $(CCCHS)^-$. (B) Charge reversal ($^-CR^+$) mass spectrum of $(CCCHS)^-$. (C) Neutralization reionization ($^-NR^+$) mass spectrum of $(CCCHS)^-$. VG ZAB 2HF mass spectrometer. For experimental conditions see Experimental Section.

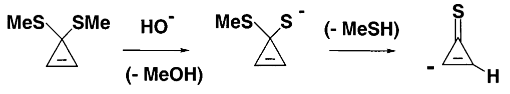

(3)

Process eq 2 involves the S_N2 (Si) nucleophilic displacement[24] of the Me_3Si group from $Me_3SiC{\equiv}CCH($*cyclo*-$S{-}C_2H_4{-}S)$ with F^- to yield $^-C{\equiv}CCH($*cyclo*-$S{-}C_2H_4{-}S)$ which then dissociates to $(CCCCHS)^-$ and SC_2H_4. The cyclic isomer $\mathbf{4}^-$ is, in principle, accessible via deprotonation of cyclopropenthione shown in eq 3. Unfortunately, this procedure was not successful: a similar strategy to produce the oxygen analogue of $\mathbf{4}^-$ from the corresponding dimethyl ketal failed previously.[21] Having formed the two anions $\mathbf{1}^-$ and $\mathbf{3}^-$, it is now necessary to demonstrate that they do not rearrange to other structures under the conditions necessary to effect electron stripping to form the neutrals **1** and **3**. The collision induced (CID) negative ion spectra (MS/MS) of the anions are shown in Figures 1a and 2a, respectively. Anion $\mathbf{1}^-$ fragments mainly by competitive losses of $H^\bullet$, $HC^\bullet$, and CS cleave in complete accord with structure $(HCCCS)^-$. In contrast, the major fragmentations of $\mathbf{3}^-$ are the losses of $H^\bullet$, C_2, and $CHS^\bullet$, in accord with structure $(CCCHS)^-$. Thus, $\mathbf{1}^-$ and $\mathbf{3}^-$ are appropriate precursors for the radicals **1** and **3** respectively.

Formation of HCCCS and CCCHS. The charge reversal [($^-CR^+$), direct conversion of the anion to the cation by synchronous two electron stripping[27,28]] and neutralization/

TABLE 3: Thermochemical Data for Decompositions of HCCCS and CCCHS Cations and Neutrals[a]

cation process	ΔH (kcal mol^{-1})	neutral process	ΔH (kcal mol^{-1})
$HCCCS^+ \rightarrow CCCS^{+\bullet} + H^\bullet$	136.4	$HCCCS^\bullet \rightarrow CCCS + H^\bullet$	63.5
$HCCCS^+ \rightarrow HCCC^+ + S$	180.6	$HCCCS^\bullet \rightarrow HCCC^\bullet + S$	136.4
$HCCCS^+ \rightarrow HCC^\bullet + CS^{+\bullet}$	170.2	$HCCCS^\bullet \rightarrow HCC^\bullet + CS$	71.7
$HCCCS^+ \rightarrow HCC^+ + CS$	190.5		
$CCCHS^+ \rightarrow CCCS^{+\bullet} + H^\bullet$	138.1	$CCCHS^\bullet \rightarrow CCCS + H^\bullet$	24.6
$CCCHS^+ \rightarrow CHS^+ + CC$	146.2	$CCCHS^\bullet \rightarrow CHS^\bullet + CC$	94.3
$CCCHS^+ \rightarrow CC^{+\bullet} + CHS^\bullet$	326.5	$CCCHS^\bullet \rightarrow HCC^\bullet + CS$	32.8

[a] ΔH values were determined from the following theoretically calculated values (Hartree): $HC_3S^+ = -511.87388$; $HC_3S^\bullet = -512.13058$; $C_2CHS^+ = -511.87658$; $C_2CHS^\bullet = -512.06863$; $C_3S^{+\bullet} = -511.15723$; $C_3S = -511.53003$; $HC_3^+ = -114.02798$; $HC_3^\bullet = -114.35497$; $C_3 = -113.74731$; $HC_2^+ = -75.95193$; $HC_2^\bullet = -76.39797$; $CS^{+\bullet} = -435.20464$; $CHS^+ = -435.92734$; $CHS^\bullet = -436.19933$; $CS = -435.61841$; $C_2^{+\bullet} = -75.16825$; $C_2 = -75.73035$; $S = -397.55817$; $H^\bullet = -0.49933$ [at CCSD(T)/aug-cc-pVDZ//B3LYP/aug-cc-pVDZ level of theory including zero-point energy corrections].

reionization ($^-$NR$^+$, stepwise two electron stripping of the anion via a neutral to the corresponding cation[20]) of $(HCCCS)^-$ and $(CCCHS)^-$ are shown in Figures 1b and 2b ($^-$CR$^+$) and Figures 1c and 2c ($^-$NR$^+$). The $^-$CR$^+$ and $^-$NR$^+$ spectra of $(HCCCS)^-$ are very similar with the fragmentations (competitive losses of $H^\bullet$, $HC^\bullet$, $HC_2^\bullet$, $S^\bullet$, and CS) consistent with a decomposing cation of structure $(HCCCS)^+$. Thus, the charge stripping sequence for **1** is $(HCCCS)^- \rightarrow HCCCS^\bullet \rightarrow (HCCCS)^+$, with no rearrangement occurring at either the neutral or cation stage of the experiment. The fact that there is a pronounced peak (recovery signal) in the $^-$NR$^+$ spectrum at *m*/*z* 69 indicates that some of the doublet HCCCS species are stable for the microsecond time frame between the formation of the neutral and its ionization to the cation. The geometries of the ground-state anion **1**$^-$ and doublet **1** are similar (cf. Tables 1 and 2) and so the excess energy of the neutral as a consequence of the vertical Franck−Condon oxidation is small: the excess energy of the neutral with the anion geometry on the neutral potential surface is calculated to be 8.3 kcal mol^{-1} (at the CCSD(T)/aug-cc-pVDZ//B3LYP/aug-cc-pVDZ level). This energy is modest and should not by itself be able to cause rearrangement or decomposition of the neutrals. Because the $^-$CR$^+$ and $^-$NR$^+$ spectra shown in Figure 1, parts b and c, are very similar, the fragment cations observed in these spectra are caused by fragmentations of $(HCCCS)^+$ rather than dissociations of neutral HCCCS with subsequent ionization of the fragment neutrals. The energies required for some of these fragmentations are shown in Table 3 and demonstrate that the decomposing cations formed following vertical oxidation must have significant excess energy due to collisions after the Franck−Condon process. The energy range is 135−190 kcal mol^{-1} (see data in Table 3).

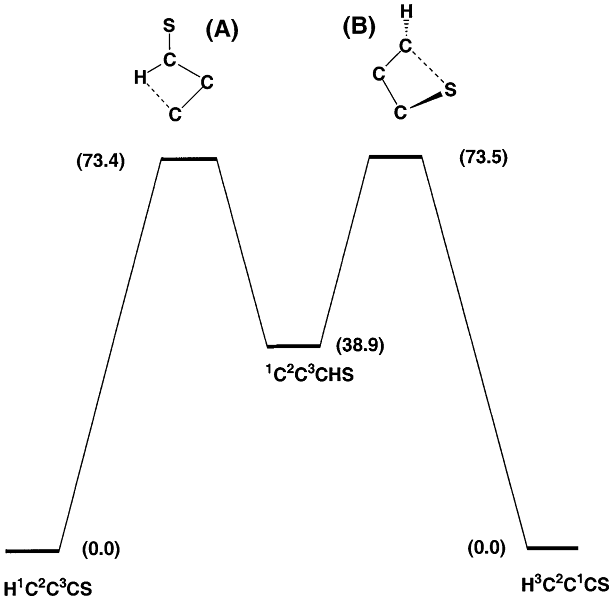

Figure 3. Concerted rearrangements of CCCHS to HCCCS via H and S migration. CCSD(T)/aug-cc-pVDZ//B3LYP/aug-cc-pVDZ level of theory. Relative energies in kcal mol^{-1} with respect to HCCCS. Full data for **1** and **3** see Table 1. Data for transition states **A** and **B** see Table 4 (Supplementary Data).

The situation with regard to the other isomer $(CCCHS)^-$ (**3**$^-$) is different. The $^-$CR$^+$ spectrum (Figure 2b) shows that (i) two-electron oxidation produces some cations of structure $(CCCHS)^+$ (suggested by peaks corresponding to losses of C, C_2 from the parent cation) and (ii) some of the initially formed species $(CCCHS)^+$ undergo rearrangement to an isomer which fragments by major losses of $CH^\bullet$ and $C_2H^\bullet$. The losses of $CH^\bullet$ and $C_2H^\bullet$ are consistent with rearrangement of $(CCCHS)^+$ to an isomer, perhaps $(HCCCS)^+$ (cf. Figure 1b)]. The $^-$NR$^+$ spectrum shown in Figure 2c is similar to the $^-$CR$^+$ spectrum, except that it shows more abundant peaks at *m*/*z* 56 ($-CH^\bullet$) and *m*/*z* 44 ($-C_2H^\bullet$) than those observed in the $^-$CR$^+$ spectrum. This means that one-electron vertical oxidation of $(CCCHS)^-$ does produce some stable neutrals corresponding to CCCHS but that some of the first-formed neutrals rearrange to an isomer. This isomer is probably the stable doublet HCCCS, but the data are also consistent with formation of the cyclic isomer **4** (see Scheme 1). The observation of rearrangement is interesting, because the similar geometries of **3**$^-$ and **3** mean that the excess Franck−Condon energy of neutral CCCHS will be small (calculated 8.4 kcal mol^{-1}), which by itself is unlikely to be sufficient to induce rearrangement of neutral CCCHS. The available data do not distinguish between the peaks at *m*/*z* 56 and 44 in the $^-$NR$^+$ spectrum (Figure 2c) being produced by (i) decompositions of the rearranged parent cation (*m*/*z* 69) or (ii) decomposition of the rearranged neutral isomer followed by ionization of the fragment neutrals C_2S and CS (cf Table 3).

Rearrangement of Neutral Doublet CCCHS. We have shown that collision-induced vertical one electron oxidation of $(HCCCS)^-$ produces a stable neutral HCCCS. In contrast, $(CCCHS)^-$ under the same experimental conditions produces some neutrals CCCHS which retain their skeletal integrity, together with others which rearrange to an isomer, possibly HCCCS (**1**) or (*cyclo*-C_3H)=S (**4**). Calculations of possible rearrangements on the C_3HS radical potential surface have been investigated at the CCSD(T)/aug-cc-pVDZ//B3LYP/aug-cc-pVDZ level of theory. These calculations have uncovered three competitive rearrangements of CCCHS (**3**) to form HCCCS (**1**), the global minimum on the potential surface. The rearrangement pathways are summarized in Figures 3 and 4. Full details of

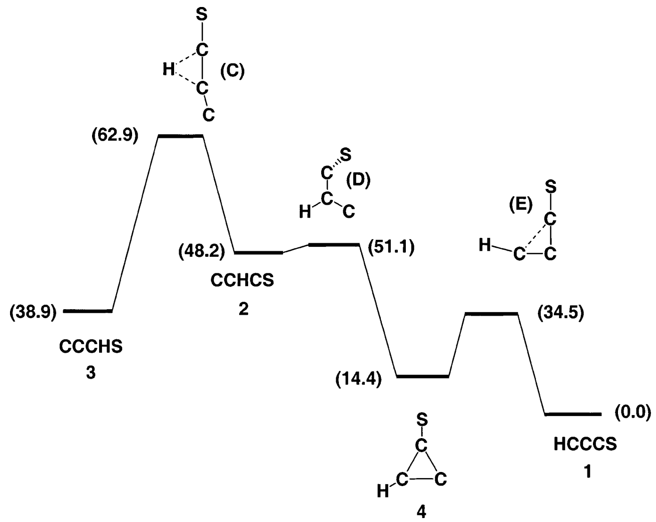

Figure 4. Stepwise rearrangement of CCCHS to HCCCS. CCSD(T)/aug-cc-pVDZ//B3LYP/aug-cc-pVDZ level of theory. Relative energies in kcal mol^{-1} with respect to that of HCCCS (0.0 kcal mol^{-1}). Full data for neutrals **1**−**4**, see Table 1. For data concerning transitions states **C** and **D**, see Table 4 (Supplementary Data).

C_3HS isomers are given in Table 1. Details of transition states shown in Figures 3 and 4 are given in Table 4 (supplementary data).

There are two concerted pathways for the conversion of CCCHS to HCCCS: these are shown in Figure 3. The first of these requires 34.5 kcal mol^{-1} to reach transition state **A** in order to effect H migration to form HCCCS. The second process involves sulfur rearrangement over transition state **B** (+34.6 kcal mol^{-1}) to also form HCCCS.[38] Both processes could, in principle, produce HCCCS with some 73 kcal mol^{-1} of excess energy. If this energy is retained by HCCCS, it is sufficient to cause decomposition by the processes (i) $HCCCS^{\bullet} \rightarrow CCCS + H^{\bullet}$ [+63.5 kcal mol^{-1} (Table 3)] and (ii) $HCCCS^{\bullet} \rightarrow HCC^{\bullet} + CS$ [+71.7 kcal mol^{-1} (Table 3)].

The third process involves the stepwise H rearrangement shown in Figure 4. This process involves all four isomers shown in Scheme 1. The first step in the sequence requires an energy of 24 kcal mol^{-1} to surmount transition state **C** and convert **3** to **2**. The radical CCHCS (**2**) then ring closes to form cyclic isomer **4** which is energized and should ring open to give HCCCS (**1**).[39] The product HCCCS could be formed with an excess energy of 62.9 kcal mol^{-1} by this reaction sequence. This is insufficient to cause decomposition of the neutral by any of the processes shown in Table 3.

Neither of the two H rearrangement processes shown in Figures 3 and 4 cause any change in the connectivity of the CCCS backbone. In contrast, the S rearrangement shown in Figure 3 causes reorganization of the CCCS backbone, namely, $C^1C^2C^3HS$ yields $HC^3C^2C^1S$. If this rearrangement does indeed involve S migration, the $^-NR^+$ spectrum of $(CC^{13}CHS)^-$ may confirm such a rearrangement. The required labeled precursor anion was synthesized as shown in eq 4

$$Me_3Si{-}C{\equiv}C{-}^{13}CH\ (cyclo\text{-}SCH_2{-}CH_2S) + F^- \rightarrow {}^-C{\equiv}C{-}^{13}CH{=}S + Me_3SiF + cyclo\text{-}SC_2H_4 \quad (4)$$

The $^-CR^+$ and $^-NR^+$ spectra of $(CC^{13}CHS)^-$ are shown in Figure 5. In accord with the data for the unlabeled species (Figure 2, parts b and c), comparison of the $^-CR^+$ and $^-NR^+$ spectra of $(CC^{13}CHS)^-$ indicate that there is more rearrangement

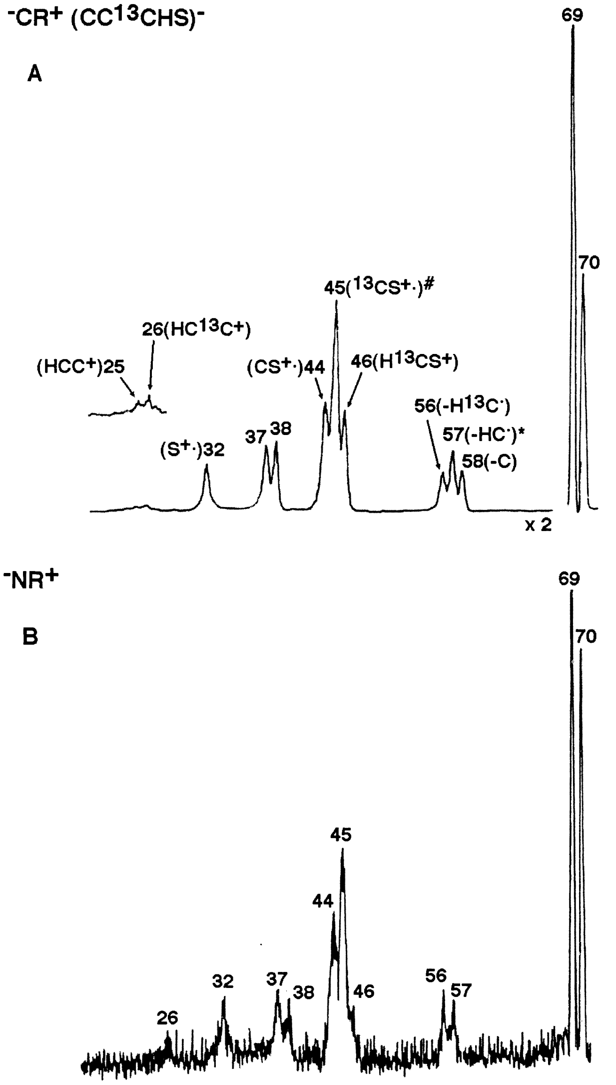

Figure 5. $^-CR^+$ (A) and $^-NR^+$ (B) spectra of $(CC^{13}CHS)^-$. VG ZAB 2HF mass spectrometer. For experimental details see Experimental section. *, see ref 40. #, see ref 41.

in the $^-NR^+$ than the $^-CR^+$ spectrum, confirming that some neutral $CC^{13}CHS$ radicals are rearranging to an isomer. The two spectra show the following peak ratios; *m/z* 57 ($-CH^{\bullet}$):[40] 56 ($-^{13}CH^{\bullet}$) [$^-CR^+$, 100:65; $^-NR^+$ 85:100]; *m/z* 45 ($-C_2H^{\bullet}$)[41]: 44 ($-C^{13}CH^{\bullet}$) [$^-CR^+$, 100:55; $^-NR^+$, 100:80], and *m/z* 26 (-CS): 25 (-^{13}CS) [$^-CR^+$ 2:3; $^-NR^+$, only *m/z* 26 is measurable; *m/z* 25 is lost in baseline noise]. Comparison of the $^-CR^+$ spectra shown in Figures 2b and 5a shows that both S [characterized by the losses of ^{13}CH, $C^{13}CH$ and CS (Figure 5a)] and H rearrangement [losses of $CH^{\bullet 40}$ and $C_2H^{\bullet 41}$ (Figure 5a)] occur during or following the formation of the positive ion $(CC^{13}CHS)^+$. The $^-NR^+$ spectrum shows more pronounced losses of $^{13}CH^{\bullet}$, $C^{13}CH^{\bullet}$, and CS than the corresponding $^-CR^+$ spectrum, indicating that the S rearrangement shown in Figure 3 occurs for neutral $CC^{13}CHS$. No conclusion can be made concerning a possible competing H rearrangement within neutral $CC^{13}CHS$ from the available experimental data. This is because we can only use direct comparisons of those peaks characteristic of S and H rearrangement, *m/z* 57:56 and 45:44, to identify the operation of S rearrangement in the neutral.

The experimental data indicate that the rearrangement of neutral CCCHS to HCCCS involves S rearrangement but provide no information concerning competing H rearrangement reactions of CCCHS. Can we obtain further data concerning the possibility of the operation of the H rearrangement reactions shown in Figures 3 and 4? Gas phase reactions are generally kinetically controlled, with the reaction rates being governed by the barrier to the transition state of the rate determining step and the probability of the reaction (the frequency factor, or preexponential Arrhenius factor[42]). The data in Figure 3 show that the barriers for the concerted H and S rearrangement processes are both close to 34.5 kcal mol^{-1}. These data alone do not differentiate between the two processes. The initial barrier of the stepwise H rearrangement is 24.1 kcal mol^{-1}, and assuming there is no entropy bottleneck for subsequent steps, this process is favored energetically. Yet we know that S rearrangement operates. Approximations of the Arrhenius factors for the concerted S and H rearrangements (Figure 3) can be determined by evaluating Q_{vib}, the relative vibrational functions for the competing transition states **A** and **B**,[21,43] and these values can be compared with that for transition state **C** for the stepwise H rearrangement shown in Figure 4.

The harmonic vibrational frequencies of each of the transition states **A**, **B**, and **C** (Figures 3 and 4) were calculated at the B3LYP/aug-cc-pVDZ level of theory using Gaussian 98. The individual values are listed in Table 5 (Supplementary Data). The values of Q_{vib} for transition states **A** and **B** are 1.96 and 1.95, respectively. The H and S concerted processes have similar barriers and similar preexponential factors for each process. Because the S rearrangement is known to occur, the theoretical data indicate that both the concerted processes shown in Figure 3 are probable. The stepwise H rearrangement has a lower barrier (to transition state **C**; 10 kcal mol^{-1} less than either concerted process). In this case, there is a difficulty in knowing precisely which of the low-frequency vibrations of **C** to use to estimate Q_{vib},[cf.43] but if all of the values listed in Table 5 are considered, the value is 4.14. These data suggest that the stepwise process should be the most favored of the three processes, provided no bottleneck occurs following the first step of the reaction shown in Figure 4.

In Conclusion. (i) The two radical neutral isomers HCCCS and CCCHS have been formed by one electron vertical oxidation from the anionic precursors $(HCCCS)^-$ and $(CCCHS)^-$ respectively. (ii) Some of the CCCHS neutrals are formed with sufficient excess energy to effect rearrangement to the more stable isomer HCCCS. Experimental evidence indicates that this process occurs, at least in part, by sulfur migration, a process shown theoretically to be exothermic by 38.9 kcal mol^{-1} but with a barrier of 34.5 kcal mol^{-1}. Theory suggests that a competing H rearrangement (either concerted or stepwise) should also convert CCCHS to HCCCS, but there is no experimental evidence to either confirm or refute this proposal.

Acknowledgment. We thank the Australian Research Council for the financial support of this project and the Australian Partnership for Advanced Computing National Facility (Canberra) for a generous allowance of super computer time. S.D. and S.P. thank the ARC for funding a research associate position and a Ph.D. scholarship, respectively, and A.M.McA acknowledges the award of an APRA Ph.D. scholarship.

Supporting Information Available: Table 4 summarizes geometry and energy data for transition state structures shown in Figures 3 and 4. Table 5 lists vibrational partition function data for Transition states **A** and **B** (Figure 3) and **C** (Figure 4). This material is available free of charge via the Internet at http://pubs.acs.org.

References and Notes

(1) http://www.cv.nrao.edu/∼awootten/allmols.html.

(2) Saito, S.; Kawaguchi, K.; Yamamoto, S.; Ohishi, M.; Suzuki, H.; Kaifu, N. *Astrophys. J. Lett.* **1987**, *317*, L115. Yamamoto, S.; Saito, S.; Kawaguchi, K.; Kaifu, N.; Suzuki, H.; Ohishi, M. *Astrophys. J. Lett*. **1987**, *317*, L121.

(3) Fuente, A.; Cernicharo, J.; Barcia, A.; Gómez-González, J. *Astron. Astrophys*. **1990**, *231*, 151.

(4) Bell, M. B.; Avery, L. W.; Feldman, P. A. *Astrophys. J*. **1993**, *417*, L37.

(5) Hirahara, Y.; Ohshima, Y.; Endo, Y. *Astrophys. J*. **1993**, *408*, L113. Kasai, Y.; Kinichi, O.; Ohshima, Y.; Hirahara, Y.; Endo, Y.; Kawaguchi, K.; Muramaki, A. *Astrophys. J*. **1993**, *410*, L45. Gordon, V. D.; McCarthy, M. C.; Apponyi, A. J.; Thaddeus, P. *Astrophys. J. Suppl. Ser*. **2001**, *134*, 311.

(6) Trimble, V. *Rev. Mod. Phys*. **1975**, *47*, 877.

(7) Brown, R. D. *Astrophys. J*. **1985**, *297*, 302. Ohishi, M.; Suzuki, H.; Ishikawa, S.; Yamada, C.; Kanamori, H.; Irvine, W. M.; Brown, R. D.; Godfrey, P. D.; Kaifu, N. *Astrophys. J*. **1991**, *380*, L39.

(8) Smith, D.; Adams, N. G.; Giles, K.; Herbst, E. *Astron. Astrophys*. **1988**, *200*, 191.

(9) Suzuki, H.; Ohishi, M.; Kaifu, N.; Kasuga, T.; Ishikawa, S.; Miyaji, T. *Vistas Astron*. **1988**, *31*, 459. Millar, T. J.; Herbst, E. *Astron. Astrophys*. **1990**, *231*, 466.

(10) Herbst, E.; Leung, C. M. *Astrophys. J. Suppl. Ser*. **1989**, *69*, 271.

(11) Howe, D. A.; Millar, T. J. *Mon. Not. R. Astron. Soc*. **1990**, *244*, 444.

(12) Smith, I. W. M. *Int. J. Mass Spectrom. Ion Processes* **1995**, *149/150*, 231. Clary, D. C.; Stoecklin, T. S.; Wickham, A. G. *J. Chem. Soc., Faraday Trans.* **1993**, *89*, 2185. Rowe, B. R.; Canosa, A.; Sims, I. R. *J. Chem. Soc., Faraday Trans*. **1993**, *89*, 2193.

(13) Petrie, S. *Mon. Not. R. Astron. Soc*. **1996**, *281*, 666 and references therein.

(14) Millar, T. J.; Flores, J. R.; Markwick, A. J. *Mon. Not. R. Astron. Soc*. **2001**, *327*, 1173.

(15) Flores, J. R.; Gómez, F. J. *J. Phys. Chem. A* **2001**, *105*, 10384. Flores, J. R.; Gómez, F. J. *Mol. Phys*. **2002,** *100*, 569.

(16) Hirahara, Y.; Ohshima, Y.; Endo, Y. *J. Chem. Phys*. **1994**, *101*, 7342.

(17) McCarthy, M. C.; Vrtilek, J. M.; Gottlieb, E. W.; Tao, F.-M.; Gottlieb, C. A.; Thaddeus, P. *Astrophys. J*. **1994**, *431*, L127.

(18) Wesdemiotis, C.; McLafferty, F. W. *Chem. Rev*. **1987**, *87*, 485.

(19) Zagorevskii, D. V.; Holmes, J. H. *Mass Spectrom. Rev*. **1994**, *13*, 133. Goldberg, N.; Schwarz, H. *Acc. Chem. Res.* **1994**, *27*, 347.

(20) For NR nomenclature, see: Schalley, C. A.; Hornung, G.; Schröder, D.; Schwarz, H. *Int. J. Mass Spectrom. Ion. Processes* **1998**, *172*, 181. Zagorevskii, D. V.; Holmes, J. L. *Mass Spectrom. Rev*. **1999**, *18*, 87.

(21) Peppe, S.; Blanksby, S. J.; Dua, S.; Bowie, J. H. *J. Phys. Chem. A* **2000**, *104*, 5817.

(22) Dawson, J. H. J.; Jennings, K. R. *J. Chem. Soc., Faraday Trans. 2* **1976**, *72*, 700.

(23) Blanksby, S. J.; Schröder, D.; Dua, S.; Bowie, J. H.; Schwarz, H. *J. Am. Chem. Soc*. **2000**, *122*, 7105.

(24) DePuy, C. H.; Bierbaum, V.; Flippin, L. A.; Grabowski, J. J.; King, G. K.; Smitt, R. J.; Sullivan, S. A. *J. Am. Chem. Soc*. **1980**, *102*, 5012.

(25) Stringer, M. G.; Bowie, J. H.; Holmes, J. L. *J. Am. Chem. Soc*. **1986**, *108*, 3888.

(26) Holmes, J. L. *Org. Mass Spectrom*. **1985**, *20*, 169.

(27) Bowie, J. H.; Blumenthal, T. *J. Am. Chem. Soc*. **1975**, *97*, 2959. Szulejko, J. E.; Bowie, J. H.; Howe, I.; Beynon, J. H. *Int. J. Mass Spectrom. Ion Phys*. **1980**, *13*, 76.

(28) Bursey, M. M. *Mass Spectrom. Rev*. **1990**, *9*, 555.

(29) Brandsma, L. *Preparative Acetylenic Chemistry*, 2nd ed.; Elsevier: New York, 1988; p 321.

(30) Furth, P. S.; Hwu, J. R. *J. Am. Chem. Soc*. **1989**, *111*, 8842.

(31) Chauvin, R. *Tetrahedron Lett*. **1995**, *36*, 401. Journet, M.; Cai, D.; DiMichele, L. M.; Larsen, R. D. *Tetrahedron Lett.* **1998**, *39*, 6427.

(32) Becke, A. D. *J. Chem. Phys*. **1993**, *98*, 5648.

(33) Stevens, P. J.; Devlin, F. J.; Chablowski, C. F.; Frische, M. J. *J. Phys. Chem*. **1994**, *98*, 11623.

(34) Dunning, T. H. *J. Chem. Phys*. **1989**, *90*, 1007. Woon, D. E.; Dunning, T. H. *J. Chem. Phys*. **1993**, *98*, 1358. Dunning, T. H.; Peterson, K. A.; Woon, D. E. Basis Sets: Correlation Consistent. In *Encyclopedia of Computational Chemistry*; Schleyer, P. v. R., Ed.; Wiley: Chichester, U.K., 1998.

(35) Frisch, M. J.; Trucks, G. W.; Schlegel, H. B.; Scuseria, G. E.; Robb, M. A.; Cheeseman, J. R.; Zakrzewski, V. G.; Montgomery, J. A., Jr.; Stratmann, R. E.; Burant, J. C.; Dapprich, S.; Millam, J. M.; Daniels, A. D.; Kudin, K. N.; Strain, M. C.; Farkas, O.; Tomasi, J.; Barone, V.; Cossi, M.; Cammi, R.; Mennucci, B.; Pomelli, C.; Adamo, C.; Clifford, S.; Ochterski, J.; Petersson, G. A.; Ayala, P. Y.; Cui, Q.; Morokuma, K.; Malick, D. K.; Rabuck, A. D.; Raghavachari, K.; Foresman, J. B.; Cioslowski, J.; Ortiz, J. V.; Stefanov, B. B.; Liu, G.; Liashenko, A.; Piskorz, P.; Komaromi, I.; Gomperts, R.; Martin, R. L.; Fox, D. J.; Keith, T.; Al-Laham, M. A.; Peng, C. Y.; Nanayakkara, A.; Gonzalez, C.; Challacombe, M.; Gill, P. M.

W.; Johnson, B. G.; Chen, W.; Wong, M. W.; Andres, J. L.; Head-Gordon, M.; Replogle, E. S.; Pople, J. A. *Gaussian 98*, revision A.9; Gaussian, Inc.: Pittsburgh, PA, 1998.

(36) Blanksby, S. J.; Dua, S.; Bowie, J. H. *J. Phys. Chem*. **1999**, *103*, 5161. To cite a particular example, the value of adiabatic electron affinity of CCCC was calculated to be 3.65 eV at the same level of theory used in this study, whereas the experimental value is 3.88 eV.[23]

(37) Lee, S. *Chem. Phys. Lett.* **1997**, *268*, 69.

(38) It has been reported[15] that there is stepwise process CCCHS (**3**) → (*cyclo*-C_3H)=S (**4**) → HCCCS (**1**). The second step of this process proceeds through a distorted rhombic transition state (barrier for the second step is 65 kcal mol^{-1} at the QCISD/6-311G** level of theory). We have not considered this process further, because it is energetically unfavorable in comparison with the concerted process shown in Figure 3.

(39) There is also the possibility of a competing decomposition of the cyclic species [(*cyclo*−C_3H)=S] (**4**) to form $HCC^{\bullet}$ and CS, a process endothermic by 18.4 kcal mol^{-1} from **4**.

(40) ^{13}C is also 13 Da, but there appears to be no way that ^{13}C could be lost directly from the $CC^{13}CHS$, $H^{13}CCCS$ or $HCC^{13}CS$ neutrals or cations.

(41) $^{12}C^{13}C$ is also 25 Da, but there appears to be no way that this fragment could lost directly from the $CC^{13}CHS$, $H^{13}CCCS$, or $HCC^{13}CS$ neutrals or cations.

(42) Okada, S.; Abe, Y.; Tanaguchi, S.; Yamabe, S. *J. Am. Chem. Soc.* **1987**, *109*, 295.

(43) McAnoy, A. M.; Dua, S.; Blanksby, S. J.; Bowie, J. H. *J. Chem. Soc., Perkin Trans. 2*, **2000**, 1665.